

Fast and high-fidelity transfer of edge states via dynamical control of topological phases and effects of dissipation

Yuuki Kanda,¹ Yusuke Fujisawa,¹ Kousuke Yakubo,^{1,2} Norio Kawakami,^{3,4,5} and Hideaki Obuse^{1,6,7,8}

¹*Department of Applied Physics, Hokkaido University, Sapporo 060-8628, Japan.*

²*National Institute of Technology, Asahikawa College, Asahikawa 071-8142, Japan*

³*Fundamental Quantum Science Program, TRIP Headquarters, RIKEN, Wako 351-0198, Japan*

⁴*Department of Physics, Ritsumeikan University, Kusatsu, Shiga 525-8577, Japan*

⁵*Department of Materials Engineering Science, Osaka University, Toyonaka, Osaka 560-8531, Japan*

⁶*Institute for Frontier Education and Research on Semiconductors, Hokkaido University, Sapporo 060-0808, Japan.*

⁷*Institute of Industrial Science, The University of Tokyo,
5-1-5 Kashiwanoha, Kashiwa, Chiba 277-8574, Japan*

⁸*The Institute for Solid State Physics, The University of Tokyo, Kashiwa, Chiba 277-8581, Japan*

(Dated: June 13, 2025)

Topological edge states are robust against symmetry-preserving perturbations and noise, making them promising for quantum information and computation, particularly in topological quantum computation through braiding operations of Majorana quasiparticles. Realizing these applications requires fast and high-fidelity dynamic control of edge states. In this work, we theoretically propose a high-fidelity method for transferring one-dimensional topological edge states by dynamically moving a domain wall between regions of different topological numbers. This method fundamentally relies on Lorentz invariance and relativistic effects, as moving the domain wall at a constant speed results in the problem into the uniform linear motion of a particle obeying a Dirac equation. We demonstrate effectiveness of our method in transferring edge states with high fidelity using a one-dimensional quantum walk with two internal states, which is feasible with current experimental technology. We also investigate how bit and phase-flip dissipation from environment affects transfer efficiency. Remarkably, these dissipation have minimal effects on efficiency at slow and fast transfer limits, respectively, which can be explained by relativistic effects to the edge states.

I. INTRODUCTION

Realizing quantum devices, such as quantum computers, requires to implement large-scale quantum information processing, which necessitates robust, high-fidelity quantum state transfer. However, quantum states are inherently unstable to decoherence. To overcome this vulnerability, various methods have been proposed in different systems, such as, coupling between atoms and photons[1, 2], spin systems [3–5], and so on[6–8].

Among various strategies, quantum state transfer utilizing edge states that emerge in topological matter is one the promising approaches [9–12], since the edge states are robust against symmetry-preserving perturbations. The edge states are localized near domain walls which are spatial boundaries where topological numbers varies in the position space [13–17].

Furthermore, edge states are also desired for the realization of topological quantum computation, a fault-tolerant approach of quantum computation utilizes Majorana quasiparticles [18, 19]. The Majorana quasiparticles are edge states that emerge in the systems such as quantum nanowires in the proximity to a superconductor realizing nontrivial topological superconductors [20–27] and Kitaev spin liquids [28–33]. In topological quantum computation, quantum logic gates are implemented by braiding these Majorana quasiparticles, which follow the non-Abelian statistics [34–38]. While faster and robust computation requires rapid movement of Majorana quasiparticles with high-fidelity [39–46], fast movement

generically reduces fidelity. Utilizing the dynamical properties of edge states under the moving domain wall should offer a superior control method to overcome this trade-off.

In this work, we theoretically propose a high-fidelity method for transferring one-dimensional topological edge states by dynamically moving a domain wall of topological numbers. We focus on a one-dimensional discrete-time quantum walk with two internal states (QW) [47–51] due to its experimental feasibility [52–62]. The QW possess nontrivial topological phases[63–67], and their topological number can be easily changed in various experiments. Therefore, we can vary the position of the domain wall by changing parameters over time and space, and then the edge states move accordingly. We specifically study the edge states of QW on a moving domain wall of the topological numbers at a constant velocity. This system can be mapped to the uniform linear motion of a particle obeying a Dirac equation[68, 69], implying that Lorentz invariance and relativistic effects govern dynamics of edge states. We propose a method for fast and high-fidelity edge states transfer by seriously taking into account these relativistic effects. Furthermore, we investigate effects of dissipation, such as bit and phase flips in the internal states of the QW, on the transfer efficiency of edge states. We reveal an intriguing dependence of transfer efficiency on the transfer velocity with dissipation. This behavior can be explained by the relativistic correlations of the internal states of the edge states.

This paper is organized as follows. In Sec. II we in-

roduce the QW considered in this work and explain the QW obeys the Dirac equation in the continuum limit. We also explain that the edge states emerge near the domain wall of the topological numbers. In Sec. III, we explain how to move the domain wall of topological numbers to transfer the edge states. We analytically calculate the wavefunctions for three types of edge states: edge states in the static system, edge states on the moving domain wall with constant velocity v in a comoving frame, and edge states moving with constant velocity v in a laboratory frame. In Sec. IV, we propose our method to rapidly transfer edge states with higher efficiency. Section V presents our numerical result, and demonstrate that the proposed method enhances the transfer efficiency of edge states and show the velocity dependence of transfer efficiency under dissipations. In Sec. VI, we summarize the contents of this paper.

II. DEFINITION OF QW AND EDGE STATE

We begin by introducing the time evolution of the QW both in the absence and presence of environmental noise. Then, we briefly explain the topological phases of the QW. To analytically show the emergence of edge states near the domain wall, we derive the effective Hamiltonian of the time-evolution operator of the QW by considering the continuum limit, and subsequently, the eigenstates of the edge state localized near the topological domain wall.

A. Time evolution of QW

The QW describes the dynamics of quantum states belonging to a Hilbert space

$$\mathcal{H} = \mathcal{H}_p \otimes \mathcal{H}_{in}, \quad (1)$$

where \mathcal{H}_p is the Hilbert space spanned by the discrete position basis $|n\rangle$, and \mathcal{H}_c is the Hilbert space corresponding to the two internal states spanned by $|L\rangle = (1 \ 0)^T$ and $|R\rangle = (0 \ 1)^T$. Therefore, the quantum state in \mathcal{H} at discrete time τ can be expressed as

$$|\psi_\tau\rangle = \sum_n \sum_{\sigma=L,R} \psi_\sigma(n, \tau) |n\rangle \otimes |\sigma\rangle, \quad (2)$$

where $\psi_\sigma(n, \tau)$ stands for the wavefunction amplitude. The time evolution of $|\psi_t\rangle$ is governed by a time evolution operator U as

$$|\psi_{\tau+1}\rangle = U |\psi_\tau\rangle. \quad (3)$$

The time evolution operator U is defined as

$$U = SC(\theta), \quad (4)$$

where S and $C(\theta)$, referred to as the shift and coin operator, respectively, are defined below:

$$S = \sum_n (|n+1\rangle \langle n| \otimes |R\rangle \langle R| + |n-1\rangle \langle n| \otimes |L\rangle \langle L|), \quad (5)$$

$$C(\theta) = \sum_n |n\rangle \langle n| \otimes \begin{pmatrix} \cos \theta & -\sin \theta \\ \sin \theta & \cos \theta \end{pmatrix}. \quad (6)$$

Note that $C(\theta)$ changes only the internal states, and S changes the positions of wavefunctions based on their internal states.

Next, we introduce the time evolution of QW in the presence of dissipations. Let ρ_τ denote the density matrix operator of the QW at time τ . In this work, we assume that the time evolution starts from a pure state $\rho_0 = |\psi_0\rangle \langle \psi_0|$ for simplicity. The time evolution is governed by the following quantum master equation for the density matrix operator,

$$\rho_{\tau+1} = (1-p)U\rho_\tau U^\dagger + pK\rho_\tau K^\dagger, \quad (7)$$

where $p \in [0, 1]$ is a real number that quantifies the strength of dissipation, and K is a Kraus operator representing dissipation. We consider dissipation affecting only the internal states of QW and we define K as

$$K_j(\phi) = \sum_n |n\rangle \langle n| \otimes e^{i\phi\sigma_j} \quad (j = x, y, z), \quad (8)$$

where $\sigma_{j=x,y,z}$ are Pauli matrices. When $j = x$, the Kraus operator $K_x(\phi)$ represents dissipation that alters the weights of internal states. In particular, $K_x(\pi/2)$ correspond to a bit flip. When $j = z$, $K_z(\phi)$ represents dephasing, a type of dissipation that introduces a phase to each components of internal states, and when $j = y$, K_y represents dissipation where both $K_x(\phi)$ and $K_y(\phi)$ coexist simultaneously.

B. Topological phase of QW and edge state

According to Ref. 66, the QW exhibits akin of a Floquet topological phase which induce zero-energy edge states and π energy edge states characterized by two topological invariants: ν_0 , associated with zero-energy edge states, and ν_π , associated with π -energy edge states. It is known that if the parameter θ is positive, $(\nu_0, \nu_\pi) = (1, 0)$, and if θ is negative, $(\nu_0, \nu_\pi) = (0, 1)$ when the time evolution operator is defined as Eq. (3). Since we focus only on the zero energy states in this work, we derive the effective Hamiltonian describing the system near zero energy through the time evolution operator which make it possible to analytically derive the eigenstate of the zero energy state.

The effective Hamiltonian H_{eff} of the QW can be defined as the generator of time evolution operator:

$$U = e^{-iH_{\text{eff}}}, \quad (9)$$

(we assume $\hbar = 1$). By taking the continuous limit of the U , we can derive the concrete form of H_{eff} [68]. Let $\tilde{U} = \tilde{S}\tilde{C}(\theta)$ be the continuous limit of $U = SC(\theta)$, and $\Psi(x, t)$ be a continuous wavefunction of the QW at the position x and at the time t ($x, t \in \mathbb{R}$). Operator \tilde{U}

represents an infinitesimal translation operator of time, thus \tilde{U} and $\Psi(x, t)$ satisfies

$$\Psi(x, t + \delta) = \tilde{U}\Psi(x, t). \quad (10)$$

where δ is a small parameter.

Next, we consider \tilde{S} and \tilde{C} , the continuous limits of the shift operator S and coin operator C . First, we discuss about \tilde{S} . Let D (D^{-1}) be the operator that translates the position of wavefunction to the left (right) infinitesimally. Using these operators, \tilde{S} can be expressed

$$\tilde{S} = \frac{1}{2}(1 + \sigma_z)D + \frac{1}{2}(1 - \sigma_z)D^{-1}. \quad (11)$$

Furthermore, D and D^{-1} satisfy the following relation

$$D\Psi(x, t) = \Psi(x - \delta, t), \quad (12)$$

$$D^{-1}\Psi(x, t) = \Psi(x + \delta, t), \quad (13)$$

respectively. By applying a Taylor expansion to the right-hand side of the above equations with respect to position x , D and D^{-1} can be described as

$$D = 1 + i\delta\hat{p}, \quad (14)$$

$$D^{-1} = 1 - i\delta\hat{p}, \quad (15)$$

where \hat{p} is a momentum operator. By substituting Eq. (14), (15) to Eq. (11),

$$\tilde{S} = e^{-i\delta\hat{p}\sigma_z} \quad (16)$$

can be obtained.

Secondly, we consider about the continuous coin operator \tilde{C} . The discrete coin operator $C(\theta)$ can be expressed using the exponential function as follow:

$$C(\theta) = e^{i\theta\sigma_y}. \quad (17)$$

Now we assume that $|\theta| \ll 1$. In this case, by performing a Taylor expansion to $C(\theta) = e^{i[\theta/\delta]\delta\sigma_y}$,

$$\tilde{C}(\theta) = 1 + i[\theta/\delta]\delta\sigma_y \quad (18)$$

can be obtained. Therefore, $\tilde{U} = \tilde{S}\tilde{C}(\theta)$ can be written as

$$\tilde{U} = 1 + i\delta\hat{p}\sigma_z + i\delta^{-1}\theta\sigma_y. \quad (19)$$

Finally, from Eq. (10) and (19), the continuous limit of time evolution equation can be expressed as

$$i\frac{\partial}{\partial t}\Psi(x, t) \equiv H_{\text{eff}}\Psi(x, t) \quad (20)$$

$$= \left[i\frac{\partial}{\partial x}\sigma_z + \delta^{-1}\theta\sigma_y \right] \Psi(x, t), \quad (21)$$

Note that Eq. (20) corresponds to the Dirac equation in (1+1) dimensions. We also note that the effective speed of light \tilde{c} is one, since the coefficient of momentum operator in Eq. (20) is one.

As we explained at the beginning of this subsection, topological numbers are changed when θ changes the sign. Therefore, we consider the following position dependent θ

$$\theta(x) = \theta_0 \tanh(ax), \quad (22)$$

to realize the domain wall of the topological numbers appears around $x = 0$, as illustrated in Fig. 1. Let $\Psi_0(x)$ be the wavefunction of edge state when the θ is defined in Eq. (22). To derive the eigenstates of the edge state analytically, we approximate $\theta(x)$ in Eq. (22) for $x \ll 1$ and H_{eff} forms

$$H_{\text{eff}} = -\hat{p}\sigma_z + \theta_0 a \delta^{-1} x \sigma_y \equiv H_{\text{eff}}^{(0)}, \quad (23)$$

and the eigenfunction for the zero-energy state $\Psi_0(x)$ satisfies

$$H_{\text{eff}}^{(0)}\Psi_0(x) = 0. \quad (24)$$

This eigenequation can be transformed into the eigenequation for the Hamiltonian of the harmonic oscillator by considering squared H_{eff} (see Appendix. A). As a result, $\Psi_0(x)$ can be derived as the Gaussian form

$$\Psi_0(x) = \frac{1}{\sqrt{2\xi\sqrt{\pi}}} \exp\left(-\frac{x^2}{2\xi^2}\right) \begin{pmatrix} 1 \\ 1 \end{pmatrix}, \quad (25)$$

where

$$\xi = \frac{1}{\sqrt{\theta_0 a \delta^{-1}}}, \quad (26)$$

represents the localization length of the edge state. The edge state in Eq. (25) is also shown in Fig. 1.

III. ANALYTICAL RESULTS OF THE WAVEFUNCTION OF MOVING EDGE STATE

Here, we analytically derive the wavefunction of an edge state on the moving topological domain wall with a constant velocity, using the effective Hamiltonian of the QW in Eq. (23) and the zero-energy edge state of the QW in Eq. (25). We note that the Lorentz invariance of the Dirac equation plays a key role in this derivation.

As mentioned previous section, the edge states of the QW appears around the domain wall. Therefore, if we define θ as

$$\theta(x, t) = \theta_0 \tanh[a(x - vt)], \quad (27)$$

and perform the time evolution with the initial state set as a zero-energy edge state, we may expect that the edge state can be transferred with the constant velocity v since

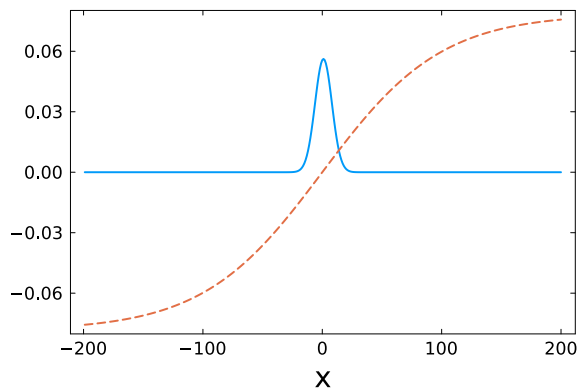


FIG. 1. $\theta(x) = \theta_0 \tanh(ax)/10$ and the edge state of QW when $\theta(x)$ is defined as such are plotted, where $\theta_0 = \pi/4$, $a = 0.01$. The dashed line represents $\theta(x)$, while the solid line represents the edge state, showing that the edge state emerges near the point where $\theta(x)$ changes its sign.

the domain wall itself moves at the velocity v . In this case, the effective Hamiltonian becomes

$$H_{\text{eff}} \equiv H_{\text{eff}}^{(v)}(x, t) = -\hat{p}\sigma_z + \theta_0\delta^{-1}a(x - vt)\sigma_y, \quad (28)$$

and the wavefunction of moving edge state $\Psi^{(v)}(x, t)$ satisfies

$$i\frac{\partial}{\partial t}\Psi^{(v)}(x, t) = H_{\text{eff}}^{(v)}(x, t)\Psi^{(v)}(x, t). \quad (29)$$

In generally, calculating $\Psi^{(v)}(x, t)$ is difficult because of the time-dependent Hamiltonian. However, in our case, the system can be mapped to the time independent system by using Lorentz invariance because our system corresponds to uniform linear motion of a particle obeying a Dirac equation. In comoving frame, i.e., a coordinate system moving at a constant velocity v along with the edge states, the wavefunction can be obtained, because the time dependence of the effective Hamiltonian is eliminated in this frame. Let (x', t') and (x, t) represent the position and time coordinates in the comoving and laboratory frame. They are related by the following Lorentz transformation:

$$x' = \gamma(x - vt) \quad (30)$$

$$t' = \gamma(t - vx), \quad (31)$$

where the Lorentz factor $\gamma = 1/\sqrt{1 - v^2}$. We remind the effective speed of light $\tilde{c} = 1$. Applying Eqs. (30) and (31), we derive the time independent Hamiltonian $H'_{\text{eff}}(x)$,

$$H'_{\text{eff}}(x) = \hat{p}\sigma_z + \theta_0\delta^{-1}\frac{a}{\gamma}x'\sigma_y. \quad (32)$$

Comparing Eq. (32) with Eq. (23) shows that the H'_{eff} replaces a with a/γ in the $H_{\text{eff}}^{(0)}$. Therefore, the wavefunction in the comoving frame $\Psi'(x')$ can be obtained

by the same substitution in eq. (25),

$$\Psi'(x') = \frac{1}{\sqrt{2\xi\sqrt{\pi/\gamma}}}\exp\left(-\frac{x'^2}{2(\xi/\sqrt{\gamma})^2}\right)\begin{pmatrix} 1 \\ 1 \end{pmatrix}. \quad (33)$$

By comparing the above equation with the wavefunction of stationary edge state, we can see that the localization length changes from ξ to $\xi\sqrt{\gamma}$. This transformation corresponds to a Lorentz contraction of localization length.

Finally, the wavefunction of moving edge state at constant velocity v in laboratory frame, $\Psi^{(v)}(x, t)$, can be derived by applying the inverse Lorentz boost to Eq. (33). Let S be the operator that transforms $\Psi'(x')$ into $\Psi^{(v)}(x, t)$ under the Lorentz boost:

$$\Psi^{(v)}(x, t) = S\Psi'(x'). \quad (34)$$

For Lorentz boosts in the x direction, S is known to take the form [70]

$$S = \exp\left[-\frac{i}{2}\eta\hat{\gamma}^0\hat{\gamma}^1\right], \quad (35)$$

where η is the rapidity, which satisfies $\eta = \text{arctanh } v$, and $\hat{\gamma}^i$ ($i = 0, 1$) is the gamma matrix. Since the gamma matrices in Eq. (29) are $\hat{\gamma}^0 = \sigma_y$ and $\hat{\gamma}^1 = i\sigma_x$, S can be written as

$$S = \exp\left[\frac{1}{2}\eta\sigma_z\right] = \sqrt{\gamma}\text{diag}(\sqrt{1+v}, \sqrt{1-v}). \quad (36)$$

Consequently, from Eqs. (34) and (36), the wavefunction of an edge state moving with velocity v can be expressed as

$$\Psi^{(v)}(x, t) = \frac{\gamma^{3/4}}{(2\xi\sqrt{\pi})^{1/2}}\exp\left[-\frac{\gamma^2(x - vt)^2}{2(\xi/\sqrt{\gamma})^2}\right]\begin{pmatrix} \sqrt{1+v} \\ \sqrt{1-v} \end{pmatrix}. \quad (37)$$

It is significant to note that the internal state of Eq. (37) depends on v , due to the relativistic effect.

IV. PROPOSAL OF THREE-STEP TRANSFER PROTOCOL

As discussed in the previous section, the edge states in QW can be transferred by defining the initial state in Eq. (25) and θ in Eq. (27), and performing time evolution. In this paper, we refer to this transfer protocol as a one-step transfer. Fig 2.(a) shows the time dependence of transfer velocity v in this method. However, non-adiabatic transitions of edge states are inevitable during transfer. To address this, we propose a protocol called a three-step transfer that reduces such transitions and enables higher-fidelity transfer. The idea to improve transfer efficiency is to gradually transform the wavefunction of stationary edge state into that of an edge state moving at velocity v before initiating its motion. As the

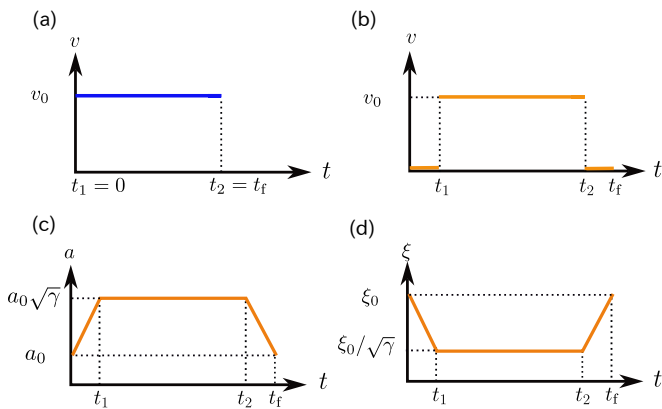


FIG. 2. Schematic diagrams of the time evolution of each parameter during edge state transfer. (a) Transfer velocity v in one-step transfer. (b) Transfer velocity v in three-step transfer. (c) Parameter a in three-step transfer. (d) Localization length ξ in three-step transfer.

name suggests, this method consists of three steps: the first step (from $\tau = 0$ to $\tau = \tau_1$), the second step (from $\tau = \tau_1$ to $\tau = \tau_2$), and the third step (from $\tau = \tau_2$ to $\tau = \tau_f$), as illustrated in Fig. 2.(b)-(d). From time $\tau = 0$ to $\tau = \tau_1$, the wavefunction of stationary edge state is gradually transformed into the wavefunction of moving edge state. From τ_1 to τ_2 , the edge state is transferred as in the one-step transfer. Finally, from τ_2 to τ_f , the inverse transformation performed from 0 to τ_1 is performed.

Now, let us discuss the specifics of the wavefunction transformation. By comparing $\Psi^0(x)$ and $\Psi^{(v)}(x, t)$, we can see that $\Psi^{(v)}(x, t)$ corresponds to changing the localization length of $\Psi_0(x)$ as $\xi \rightarrow \xi/\sqrt{\gamma}$ and modifying the internal state as $(1, 1)^T \rightarrow (\sqrt{1+v}, \sqrt{1-v})^T$. From this, the localization length transformation can be achieved through variation of the parameter a as

$$a(\tau) = a_0 + a_0(\gamma - 1) \frac{\tau}{\tau_1}, \quad (\tau \in [0, \tau_1]). \quad (38)$$

Here, we assume that $a = a_0$ in the initial state, which correspond to the stationary edge state. A larger τ_1 leads a more adiabatic parameter change. Additionally, the desired transformation of the internal state can be achieved by applying the following operator to the initial state:

$$C_v = \begin{pmatrix} \sqrt{1+v} + \sqrt{1-v} & \sqrt{1+v} - \sqrt{1-v} \\ -\sqrt{1+v} + \sqrt{1-v} & \sqrt{1+v} + \sqrt{1-v} \end{pmatrix}. \quad (39)$$

Then, in third-step, the inverse of the transformation that explained above is performed.

V. NUMERICAL RESULTS

In this section, we demonstrate the efficiency of our proposed method to transfer the edge state. To this end, we first define fidelity as a measure of the transfer efficiency of edge states. Then, we present the transfer-

velocity dependence of the fidelity in the absence and presence of dissipation.

Consider the case where the edge state is transferred over a distance of vt_f . In this case, fidelity, or transfer efficiency, is defined as follow [71]

$$F = \text{Tr} \left[\sqrt{\rho_f(x, t_f)} \sqrt{\rho_0(x - vt_f)} \right] \quad (40)$$

where $\rho_f(x, t_f)$ is the density operator of the end state of the edge state, and $\rho_0(x - vt_f)$ is the density operator of the initial state of the edge state, shifted by a distance vt_f . Fidelity F takes a value between zero and one, with a value closer to one indicating higher transfer efficiency of the edge state. In particular, when we consider only the pure states, F can be expressed using state vector,

$$F = |\langle \psi_f(x, t_f) | \Psi_0(x - vt_f) \rangle|. \quad (41)$$

A. Transfer without dissipation

In this subsection, we compare the fidelity of zero-energy edge state transferred using Eqs. (3) and (27) with the three-step and the one-step transfer methods. Fig. 3 shows the velocity dependence of fidelity when edge state is transferred using each of the two methods. Note that the vertical axis represents $1 - F$, where smaller values indicate higher fidelity, and the horizontal axis represents $w = (t_2 - t_1)v/t_f$. This correction is necessary for a fair comparison of transfer efficiency because the two methods involve different distances over which edge states can be transferred within the same time. Fig. 3 shows that our proposed method increases the fidelity of edge state transfer. In particular, for not too large v , the efficiency increases dramatically, by a factor 10^2 to 10^3 . It also shows that the smaller the values of v , a , and θ_0 , the higher transfer efficiency. This is because a smaller v results in less change in the wavefunction, while a smaller a and θ_0 improves the accuracy of the continuum approximation, this leads to an improvement in the effectiveness of the correction in the three-step transfer protocol.

B. Transfer with dissipation

Figure. 4 shows the transfer efficiency of edge states under three-step transfer with dissipation using Eqs. (7) and (27). As expected intuitively, dissipation reduces transfer efficiency, and as p increases, meaning stronger dissipation, the efficiency decreases. If we consider about ϕ , we find that the closer ϕ is to $\pi/2$, the lower transfer efficiency. Additionally, in particular, it is observed that bit flip dissipation has little effect on transfer efficiency when v is small, while dephasing dissipation has little effect when v is large. The cause of these behaviors can be explained by considering the internal state of the wavefunction of moving edge state. In laboratory frame,

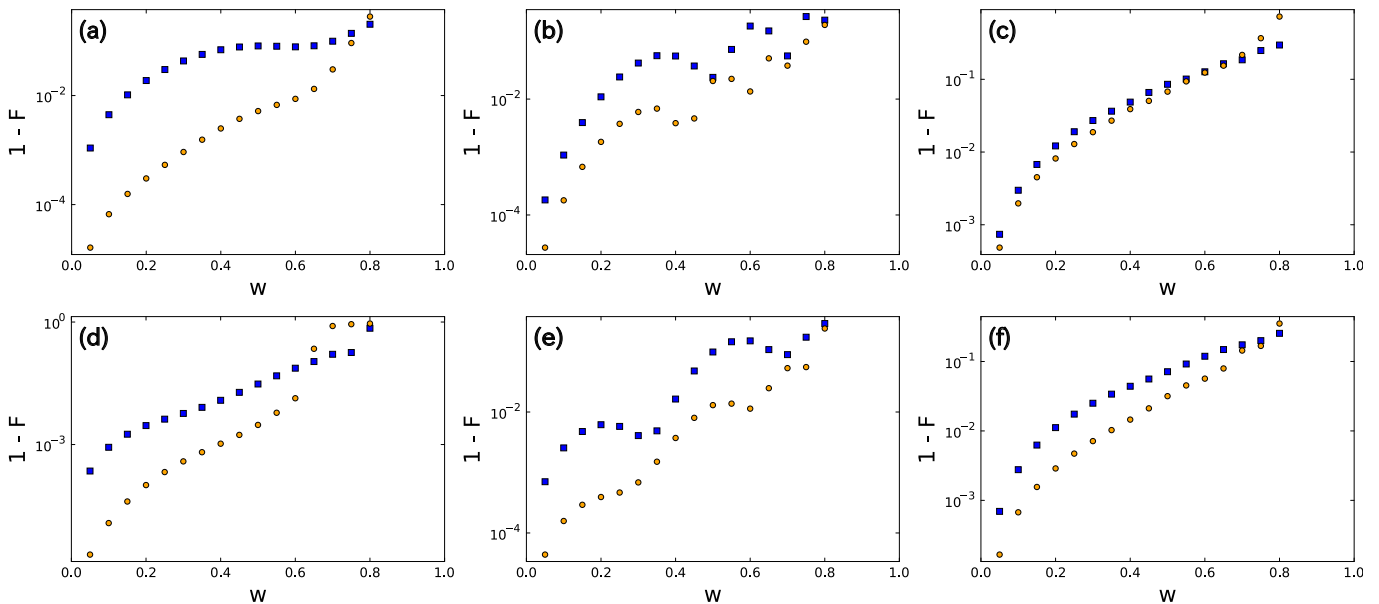


FIG. 3. Transfer velocity dependence of transfer efficiency for edge states using one-step and three-step transfer protocol. The vertical axis represents $1 - F$, where smaller values indicate higher fidelity, and the horizontal axis represents $w = (t_2 - t_1)v/t_f$ for a fair comparison between two methods. For three-step transfer, $t_1 = 10$, $t_2 = 110$, and $t_f = 120$, while for one-step transfer, $t_1 = 0$ and $t_2 = t_f = 100$. Square markers represent the results for one-step transfer, and circle markers represent those for three-step transfer. (a) $\theta_0 = \pi/6, a = 0.01$. (b) $\theta_0 = \pi/6, a = 0.1$. (c) $\theta_0 = \pi/6, a = 1.0$. (d) $\theta_0 = \pi/12, a = 0.01$. (e) $\theta_0 = \pi/12, a = 0.1$. (f) $\theta_0 = \pi/12, a = 1.0$.

when v is small enough, the internal state of the moving edge state satisfies

$$\begin{pmatrix} \sqrt{1+v} \\ \sqrt{1-v} \end{pmatrix} \rightarrow \begin{pmatrix} 1 \\ 1 \end{pmatrix}, \quad (42)$$

which is an eigenvector of σ_x belonging to the eigenvalue one. In other words, when v is small enough, the wavefunction of moving edge state is also an eigenfunction of σ_x , meaning that bit flip dissipation has little impact on the transfer efficiency. Note that this property is ensured by chiral symmetry in the context of topological insulators: edge states are also the eigenstates of the unitary operator Γ , which satisfies $\Gamma H \Gamma^{-1} = -H$, representing chiral symmetry. Similarly, when v is large enough, or close to $\tilde{c} = 1$, the internal state of the moving edge state becomes

$$\begin{pmatrix} \sqrt{1+v} \\ \sqrt{1-v} \end{pmatrix} \rightarrow \sqrt{2} \begin{pmatrix} 1 \\ 0 \end{pmatrix}, \quad (43)$$

which is an eigenvector of σ_z belonging to the eigenvalue one. In other words, when v is large enough, the wavefunction of moving edge state becomes an eigenfunction of σ_z , meaning that dephasing dissipation no longer affects the transfer efficiency. This property is ensured by the Lorentz invariance of Dirac equation.

VI. SUMMARY

In this work, we theoretically proposed a high-fidelity method for transferring one-dimensional topological edge states by dynamically moving the topological domain wall. To this end, understanding the dynamical properties of edge states is required. Taking the advantage of experimental feasibility, we focused on the one-dimensional QW with two internal degrees of freedom. By considering the continuum limit and Lorentz invariance, we derived the wavefunction of the edge states on the moving domain wall with the constant velocity. We then we proposed the three-step transfer method which can reduce the excitations to other states by accounting for Lorentz contraction of the localization length of the edge states. Our numerical calculation confirmed the efficiency of the three-step transfer method by comparing with the naive one-step transfer method. Furthermore, we investigated the velocity dependence of transfer efficiency under dissipations. We find that a bit flip dissipation has minimal effects when the transfer velocity v is small, while the effects of dephasing dissipation becomes weak with increasing v . These behaviors can be explained by the velocity-dependent internal state of the edge state, which stems from relativistic effects.

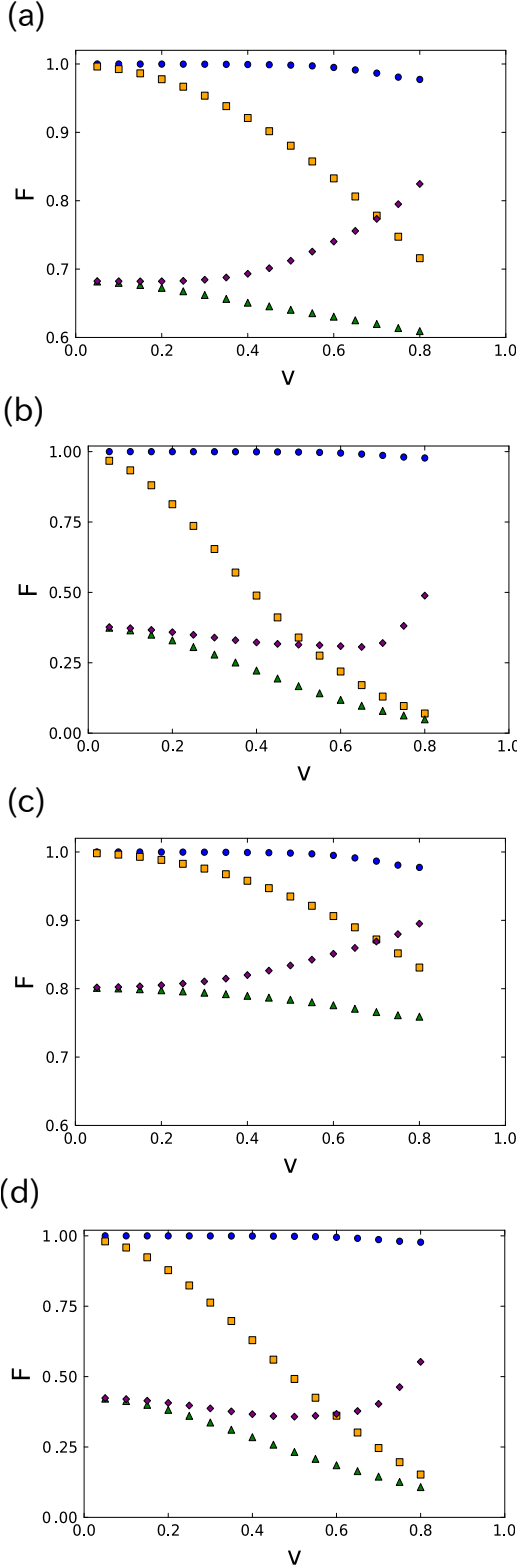


FIG. 4. v -dependence of transfer efficiency when edge states are transferred with dissipation using three-step transfer method. Note that $\theta_0 = \pi/4$, $a = 0.01$, $t_1 = 10$, $t_2 = 110$, and $t_f = 120$. Round markers represent the no-dissipation case, square markers correspond to bit flip dissipation, diamond markers indicate dephasing dissipation, and triangle markers represent the case where both bit flip and dephasing dissipation are present. (a) $\phi = \pi/2$ and $p = 0.01$. (b) $\phi = \pi/2$ and $p = 0.1$. (c) $\phi = \pi/4$ and $p = 0.01$. (d) $\phi = \pi/4$ and $p = 0.1$.

ACKNOWLEDGMENTS

We thank Y. Asano, T. Sano, and A. Sasaki for their helpful discussions. This work was supported by JSPS KAKENHI (Grants No. JP23K22411 and No. JP24K00545). H.O. was supported by JST PRESTO Grant No. JPMJPR2454. N.K. was supported by the RIKEN TRIP initiative.

Appendix A: derivation of the Eq.(25)

In this section, we derive Eq. (25). The calculation method is based on a paper that discusses unitary-equivalent Hamiltonians in relation to the effective Hamiltonian of QW [39].

Since θ is time-independent, we consider the Schrödinger equation for the steady state:

$$H_{\text{eff}}\Psi(x) = E\Psi(x). \quad (\text{A1})$$

Now, squaring H_{eff} gives

$$H_{\text{eff}}^2 = \hat{p}^2 + (\theta_0 a \delta^{-1})^2 \hat{x}^2 + \theta_0 a \delta^{-1} \sigma_x. \quad (\text{A2})$$

$$= H_0^2 + \theta_0 a \delta^{-1} \sigma_x, \quad (\text{A3})$$

where H_0 corresponds to the Hamiltonian of the harmonic oscillator. Furthermore, for simplicity, we perform the unitary rotation to H_{eff}^2 with $X = e^{i\pi\sigma_y/4}$. Then

$$\tilde{H}_{\text{eff}}^2 = X H_{\text{eff}}^2 X^\dagger \quad (\text{A4})$$

$$= \tilde{H}_0^2 + \theta_0 a \delta^{-1} \sigma_z, \quad (\text{A5})$$

can be obtained. Let $\tilde{\Psi}(x) = (\psi(x), \varphi(x))^T$ be the two-component eigenfunction of \tilde{H}_{eff} . $\tilde{\Psi}(x)$ satisfies the following eigenvalue equation

$$\tilde{H}_{\text{eff}}^2 \tilde{\Psi}(x) = E_n^2 \tilde{\Psi}(x). \quad (\text{A6})$$

From Eqs. (A4) and (A6), each of the components follows the equation

$$\begin{cases} \tilde{H}_0^2 \psi(x) = (E_n^2 - \theta_0 a \delta^{-1}) \psi(x) \\ \tilde{H}_0^2 \varphi(x) = (E_n^2 + \theta_0 a \delta^{-1}) \varphi(x). \end{cases} \quad (\text{A7})$$

We can find that $\psi(x)$ and $\varphi(x)$ are also the eigenfunction of \tilde{H}_0^2 . Thus, $\tilde{\Psi}(x)$ can be represented as

$$\tilde{\Psi}(x) = \begin{pmatrix} \phi_n(x) \\ \phi_m(x) \end{pmatrix} \quad (\text{A8})$$

Here $\psi_n(x)$ is an eigenfunction of the Hamiltonian of harmonic oscillator \tilde{H}_0^2 with the corresponding eigenvalue $E_0^{2(n)}$, where they are given

$$E_0^{2(n)} = \omega \left(n + \frac{1}{2} \right), \quad (\text{A9})$$

$$\phi_n(x) = C_n \mathcal{H}_n \exp\left[-\frac{x^2}{2\xi^2}\right]. \quad (\text{A10})$$

Remark that $\omega = 2\theta_0 a \delta^{-1}$, C_n is the normalization constant and \mathcal{H}_n is the Hermite polynomial. By applying Eq. (A8) to Eq. (A7), we obtain $n = (m - 1)$. Thus, $\tilde{\Psi}(x)$ can be written as

$$\tilde{\Psi}(x) = \begin{pmatrix} \phi_{n-1}(x) \\ \phi_n(x) \end{pmatrix}. \quad (\text{A11})$$

Note that if the subscript of the wavefunction is negative, the corresponding component is zero. Substituting Eq. (A11) to Eq. (A7), the eigenenergy E_n can be obtained as

$$E_n = \sqrt{\omega|n|}. \quad (\text{A12})$$

This indicates that the wavefunction of the zero-energy edge state corresponds to the case where $n = 0$. In other words, the wavefunction of the zero-energy state can be written as

$$\tilde{\Psi}_0(x) = C_0 \exp\left[-\frac{x^2}{2\xi^2}\right] \begin{pmatrix} 0 \\ 1 \end{pmatrix}. \quad (\text{A13})$$

By applying X to both sides of Eq. (A2), we can see that the eigenfunction of H_{eff} can be represented as

$$\Psi_0(x) = X \tilde{\Psi}_0(x) \quad (\text{A14})$$

$$= \frac{1}{\sqrt{2\xi\sqrt{\pi}}} \exp\left(-\frac{x^2}{2\xi^2}\right) \begin{pmatrix} 1 \\ 1 \end{pmatrix}. \quad (\text{A15})$$

-
- [1] J. I. Cirac, P. Zoller, H. J. Kimble, and H. Mabuchi, *Phys. Rev. Lett.* **78**, 3221 (1997).
- [2] D. N. Matsukevich and A. Kuzmich, *Science* **306**, 663 (2004).
- [3] S. Bose, *Phys. Rev. Lett.* **91**, 207901 (2003).
- [4] M. Christandl, N. Datta, A. Ekert, and A. J. Landahl, *Phys. Rev. Lett.* **92**, 187902 (2004).
- [5] Z. Song and C. P. Sun, *Low Temperature Physics* **31**, 686 (2005).
- [6] L. Tian, *Annalen der Physik* **527**, 1 (2015).
- [7] B. Vermersch, P.-O. Guimond, H. Pichler, and P. Zoller, *Phys. Rev. Lett.* **118**, 133601 (2017).
- [8] Z.-L. Xiang, M. Zhang, L. Jiang, and P. Rabl, *Phys. Rev. X* **7**, 011035 (2017).
- [9] N. Yao, C. Laumann, *et al.*, *Nature Communications* **4**, 1585 (2013).
- [10] C. Dłaska, B. Vermersch, and P. Zoller, *Quantum Science and Technology* **2**, 015001 (2017).
- [11] B. H. Lang, N, *npj Quantum Inf* **3**, 10.1038/s41534-017-0047-x (2017).
- [12] F. Mei, G. Chen, L. Tian, S.-L. Zhu, and S. Jia, *Phys. Rev. A* **98**, 012331 (2018).
- [13] C. L. Kane and E. J. Mele, *Phys. Rev. Lett.* **95**, 146802 (2005).
- [14] C. L. Kane and E. J. Mele, *Phys. Rev. Lett.* **95**, 226801 (2005).
- [15] M. Z. Hasan and C. L. Kane, *Rev. Mod. Phys.* **82**, 3045 (2010).
- [16] X.-L. Qi and S.-C. Zhang, *Rev. Mod. Phys.* **83**, 1057 (2011).
- [17] X.-G. Wen, *Rev. Mod. Phys.* **89**, 041004 (2017).
- [18] A. Y. Kitaev, *Physics-Uspekhi* **44**, 131 (2001).
- [19] A. Kitaev and C. Laumann (2009) arXiv:0904.2771 [cond-mat.mes-hall].
- [20] D. A. Ivanov, *Phys. Rev. Lett.* **86**, 268 (2001).
- [21] R. G. e. a. Alicea, *J. Phys. X*, **7**, 412 (2011).
- [22] L. Fu and C. L. Kane, *Phys. Rev. Lett.* **100**, 096407 (2008).
- [23] Y. Oreg, G. Refael, and F. von Oppen, *Phys. Rev. Lett.* **105**, 177002 (2010).
- [24] R. M. Lutchyn, J. D. Sau, and S. Das Sarma, *Phys. Rev. Lett.* **105**, 077001 (2010).
- [25] A. J. Rep. Prog. Phys. **75**, 076501 (2012).
- [26] S. F. M. Sato, *J. Phys. Soc. Jpn.* **85**, 072001 (2016).
- [27] C. W. J. Beenakker, *SciPost Phys. Lect. Notes* , 15 (2020).
- [28] A. Kitaev, *Annals of Physics* **321**, 2 (2006), january Special Issue.
- [29] L. Balents, *Nature* **464**, 199 (2010).
- [30] L. Savary and L. Balents, *Reports on Progress in Physics* **80**, 016502 (2016).
- [31] J. Knolle and R. Moessner, *Annual Review of Condensed Matter Physics* **10**, 451 (2019).
- [32] C. Balz, L. Janssen, P. Lampen-Kelley, A. Banerjee, Y. H. Liu, J.-Q. Yan, D. G. Mandrus, M. Vojta, and S. E. Nagler, *Phys. Rev. B* **103**, 174417 (2021).
- [33] J. Nasu, *Progress of Theoretical and Experimental Physics* **2024**, 08C104 (2023).
- [34] C. Nayak, S. H. Simon, A. Stern, M. Freedman, and S. Das Sarma, *Rev. Mod. Phys.* **80**, 1083 (2008).
- [35] N. C. Sarma, S. Freedman, M, *npj Quantum Inf* **1**, 15001 (2015).
- [36] T. Karzig, C. Knapp, R. M. Lutchyn, P. Bonderson, M. B. Hastings, C. Nayak, J. Alicea, K. Flensberg, S. Plugge, Y. Oreg, C. M. Marcus, and M. H. Freedman, *Phys. Rev. B* **95**, 235305 (2017).
- [37] V. Lahtinen and J. K. Pachos, *SciPost Phys.* **3**, 021 (2017).
- [38] P. Marra, *Journal of Applied Physics* **132**, 231101 (2022), https://pubs.aip.org/aip/jap/article-pdf/doi/10.1063/5.0102999/19874157/231101_1.5.0102999.pdf.
- [39] T. Karzig, G. Refael, and F. von Oppen, *Phys. Rev. X* **3**, 041017 (2013).
- [40] T. Karzig, F. Pientka, G. Refael, and F. von Oppen, *Phys. Rev. B* **91**, 201102 (2015).
- [41] T. Karzig, A. Rahmani, F. von Oppen, and G. Refael, *Phys. Rev. B* **91**, 201404 (2015).
- [42] C. S. Amorim, K. Ebihara, A. Yamakage, Y. Tanaka, and M. Sato, *Phys. Rev. B* **91**, 174305 (2015).
- [43] S. Longhi, *Phys. Rev. B* **99**, 155150 (2019).
- [44] F. M. D'Angelis, F. A. Pinheiro, D. Guéry-Odelin, S. Longhi, and F. m. c. Impens, *Phys. Rev. Res.* **2**, 033475 (2020).

- [45] S. V. Romero, X. Chen, G. Platero, and Y. Ban, *Phys. Rev. Appl.* **21**, 034033 (2024).
- [46] F. Yu, P. Z. Zhao, and J. Gong, Nonadiabatic braiding of majorana modes (2025), arXiv:2503.00953 [quant-ph].
- [47] Y. Aharonov, L. Davidovich, and N. Zagury, *Phys. Rev. A* **48**, 1687 (1993).
- [48] D. A. Meyer, *Journal of Statistical Physics* **85**, 551 (1996).
- [49] J. Kempe, *Contemporary Physics* **44**, 307 (2003), <https://doi.org/10.1080/00107151031000110776>.
- [50] A. Ambainis, *SIAM Journal on Computing* **37**, 210 (2007), <https://doi.org/10.1137/S0097539705447311>.
- [51] T. Kitagawa, M. A. Broome, A. Fedrizzi, M. S. Rudner, E. Berg, I. Kassal, A. Aspuru-Guzik, E. Demler, and A. G. White, *Nature Communications* **3**, 10.1038/ncomms1872 (2012).
- [52] P. L. Knight, E. Roldán, and J. Sipe, *Optics Communications* **227**, 147 (2003).
- [53] P. L. Knight, E. Roldán, and J. E. Sipe, *Phys. Rev. A* **68**, 020301 (2003).
- [54] H. Jeong, M. Paternostro, and M. S. Kim, *Phys. Rev. A* **69**, 012310 (2004).
- [55] E. Roldán and J. C. S. and, *Journal of Modern Optics* **52**, 2649 (2005).
- [56] A. Rai, G. S. Agarwal, and J. H. H. Perk, *Phys. Rev. A* **78**, 042304 (2008).
- [57] L. Sansoni, F. Sciarrino, G. Vallone, P. Mataloni, A. Crespi, R. Ramponi, and R. Osellame, *Phys. Rev. Lett.* **108**, 010502 (2012).
- [58] A. Crespi, R. Osellame, R. Ramponi, V. Giovannetti, R. Fazio, L. Sansoni, F. De Nicola, F. Sciarrino, and P. Mataloni, *Nature Photonics* **7**, 322 (2013).
- [59] H. Schmitz, R. Matjeschk, C. Schneider, J. Glueckert, M. Enderlein, T. Huber, and T. Schaetz, *Phys. Rev. Lett.* **103**, 090504 (2009).
- [60] M. Karski, L. Förster, J.-M. Choi, A. Steffen, W. Alt, D. Meschede, and A. Widera, *Science* **325**, 174 (2009).
- [61] F. Zähringer, G. Kirchmair, R. Gerritsma, E. Solano, R. Blatt, and C. F. Roos, *Phys. Rev. Lett.* **104**, 100503 (2010).
- [62] R. Matjeschk, C. Schneider, M. Enderlein, T. Huber, H. Schmitz, J. Glueckert, and T. Schaetz, *New Journal of Physics* **14**, 035012 (2012).
- [63] T. Kitagawa, M. S. Rudner, E. Berg, and E. Demler, *Phys. Rev. A* **82**, 033429 (2010).
- [64] H. Obuse and N. Kawakami, *Phys. Rev. B* **84**, 195139 (2011).
- [65] T. Kitagawa, *Quantum Information Processing* **11**, 1107 (2012).
- [66] J. K. Asbóth and H. Obuse, *Phys. Rev. B* **88**, 121406 (2013).
- [67] K. Mochizuki, T. Bessho, M. Sato, and H. Obuse, *Phys. Rev. B* **102**, 035418 (2020).
- [68] F. W. Strauch, *Phys. Rev. A* **73**, 054302 (2006).
- [69] P. Arrighi, G. Di Molfetta, I. Márquez-Martín, and A. Pérez, *Phys. Rev. A* **97**, 062111 (2018).
- [70] J. Sakurai, *Advanced Quantum Mechanics*, Always learning (Pearson Education, Incorporated, 1967).
- [71] A. Uhlmann, *Reports on Mathematical Physics* **9**, 273 (1976).